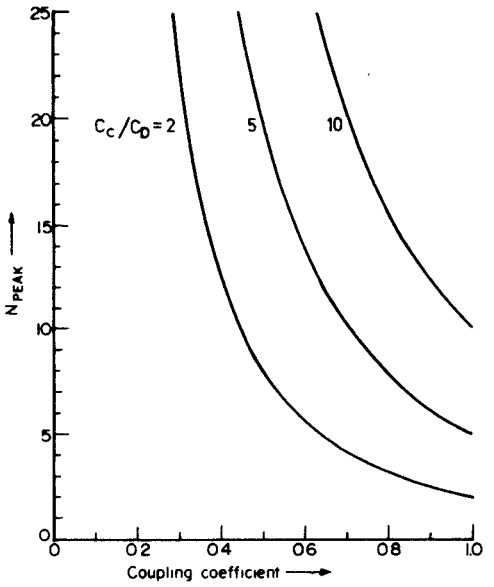

Fig. 2. N_{peak} as a function of coupling coefficient n_t. The parameter is the C_c/C_D ratio.

oscillator of high power-combining efficiency, after a few devices are added, the rms frequency deviation may be expected to decrease rapidly as the active devices are further increased in number. However, much depends on the C_c/C_D ratio. If this ratio is small, the rms frequency deviation may fall without undergoing any rise when the active devices are increased in number. For example, when the C_c/C_D ratio is 2 and the coupling coefficient is 1.0, N_{peak} is 2 (Fig. 2). In such a case, as the active devices of the multiple-device oscillator are increased in number from the minimum of 2, the rms frequency deviation only decreases and does not rise at all. On the other hand, if the coupling coefficient is small and the C_c/C_D ratio is large enough for N_{peak} to be larger than the maximum number of devices that can be accommodated by the oscillator structure, the rms frequency deviation continues to increase as the active devices are increased in number. The curve for $n_t = 0.2$ in Fig. 1 is such an example of a multiple-device oscillator structure with fewer than 15 devices.

If the active devices are increased in number to the extent that

$$n_t^2 N g_{opt} \gg G_c \tag{10}$$

and

$$n_t^2 N C_D \gg C_c \tag{11}$$

then from (8)

$$\Delta f_{rms} \simeq \frac{g_{opt}}{2\pi C_D}\sqrt{\frac{\overline{v_n^2}\, g_{opt}}{4NP_d}} \tag{12}$$

Thus as shown by (12), when a multiple-device oscillator is comprises a very large number of active devices, its rms frequency deviation is independent of the coupling coefficient and is inversely proportional to the square root of the number of constituent active devices.

III. Conclusions

Considering the dependence of external Q on circuit and active device parameters, an analysis of FM noise in a multiple-device oscillator is presented. The analysis shows that, with proper selection of circuit parameters, the rms frequency deviation in such an oscillator decreases rapidly with an increase in the number of active devices. Increased coupling between the active devices and the power-combining cavity increases the rms frequency deviation. This influence of device–cavity coupling, however, diminishes as the active devices are increased in number.

References

[1] K. Kurokawa, "The single-cavity multiple-device oscillators," *IEEE Trans. Microwave Theory Tech.*, vol. MTT-19, pp. 793–801, Oct 1971.
[2] R. Aston, "Techniques for increasing the bandwidth of a TM_{010}-mode power combiner," *IEEE Trans. Microwave Theory Tech*, vol. MTT-27, pp. 479–482, May 1979.
[3] Y.E Ma and C Sun, "1-W millimeter-wave Gunn diode combiner," *IEEE Trans. Microwave Theory Tech.*, vol. MTT-28, pp. 1460–1463, Dec 1980.
[4] S. Nogi and K. Fukui, "Locking behavior of a microwave multiple-device ladder oscillator," *IEEE Trans. Microwave Theory Tech.*, vol. MTT-33, pp. 253–262, Mar 1985.
[5] S. Sarkar and O.S Gupta, "Dependence of multiple-device oscillator injection locking range on the number of constituent devices," *IEEE Trans. Microwave Theory Tech.*, vol. MTT-34, pp 839–840, July 1986.
[6] J. Josenhans, "Noise spectra of Read diode and Gunn oscillators," *Proc. IEEE*, vol. 54, pp. 1478–1479, Oct. 1966.

Measurements of Microstrip Effective Relative Permittivities

STEVE DEIBELE, STUDENT MEMBER, IEEE,
AND JAMES B. BEYER, SENIOR MEMBER, IEEE

***Abstract*—This paper presents normalized wide-bandwidth measurements of microstrip effective relative permittivities (ϵ_{eff}) which were made on large-scale microstrip models. The experimental techniques are discussed, and the data are compared to the predictions of two recent closed-form design equations. These results agree favorably with the predictions of Kirschning and Jansen's model. In addition, suggestions concerning frequency limitations of microstrip use and comments on the reliability of CAD packages for microstrip circuits are made.**

I. Introduction

Increased interest has recently been expressed in the characterization of microstrip, one of the popular planar transmission lines. Microstrip does not support transverse electromagnetic (TEM) waves and is hence dispersive. Several researchers [1]–[6] have employed both approximate and rigorous numerical techniques to calculate the phase velocities and the "impedances," but the rigorous techniques are quite involved and require too much computer time to be used directly in computer-aided design (CAD) applications [7]. Furthermore, the approximate techniques have limited regions of validity. Recently, two groups of researchers, Kirschning and Jansen [7] and Hammerstad and Jensen [8], addressed this problem by providing closed-form

Manuscript received September 29, 1986; revised January 17, 1987. This work was supported in part by the Hewlett-Packard Company, Stanford Park Division.

The authors are with the Department of Electrical and Computer Engineering, University of Wisconsin, Madison, WI 53706.

IEEE Log Number 8613831.

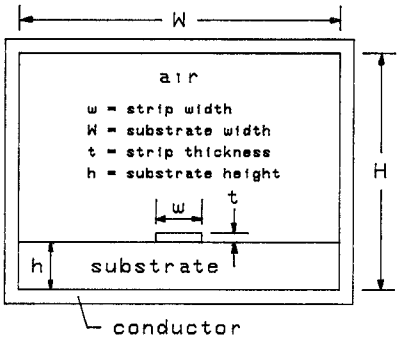

Fig. 1. The cross section of a typical shielded microstrip line (not to scale) The substrate is characterized by μ_0 and $\epsilon_r\epsilon_0$ where $\epsilon_r > 1$.

design equations of the effective relative permittivity (ϵ_{eff}), but beyond low (normalized) frequencies the predictions of these two equations deviate significantly from one another. Only a few experimental data sets limited to intermediate normalized frequencies are available for comparison to these and other design equations, leaving the microstrip circuit engineer uncertain which of the microstrip models and the respective closed-form dispersion design equations to use. For example, the experimental data sets published in [5], [6], and [9] remain below (frequency)(substrate height) $\triangleq fh = 1.6$ GHz-cm. To remedy that situation, this paper presents the needed wide-bandwidth (up to $fh = 4$ GHz-cm) measurements of the microstrip effective relative permittivity on three experimental circuits. Comparisons of those data with the ϵ_{eff} predictions of [7] and [8] are made. The experimental data points closely follow the predictions of [7] across a very wide bandwidth and support those of [8] only near the lower (normalized) frequencies.

Microstrip Geometry and Notation

Fig. 1 depicts the standard notation used for describing microstrip parameters. In this paper, ϵ_r denotes the substrate relative permittivity. Because no magnetic materials are employed in the experimental circuits, the relative permeabilities μ_r of the dielectrics and the conductors are assumed to be unity. Ideally, the cross-sectional dimensions H and W are very large relative to both the substrate height h and the strip width w. The presence (or absence) of the top and side shielding conductors then negligibly affects the microstrip behavior as compared to the case involving infinite dimensions for H and W.

II. The Experimental Apparatus and the Measurement Scheme [10]

Three large-scale microstrip circuits using substrate relative permittivities near 9 and strip-width-to-substrate-height ratios (w/h) in the range $0.4 < w/h < 2$ were analyzed. The circuit substrates were cut from a single quarter inch ($\doteq 0.6$ cm) thick sheet of Emerson-Cuming's stycast high-K dielectric, a low-loss, machinable material designed for microwave use. The advantages of using large-scale circuits include the possibility of creating unique circuit layouts in-house, having greater tolerances of machining and parts layouts, and above all, being able to use lower test frequencies where accurate measurement equipment is readily available. Appropriately configured layers of plated copper formed the single-strip circuits. The microstrips were short-circuited on each end, creating resonant structures. The resonance measurement method described by Getsinger [1] was used to determine the effective relative permittivity ϵ_{eff} (or, equivalently, the phase velocity) at discrete frequency points. This method and the details of the constructions are described below.

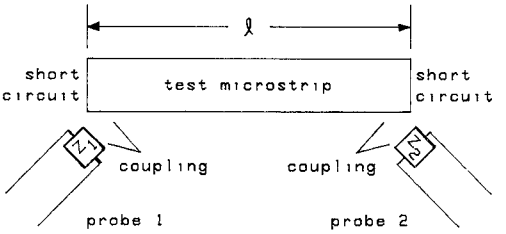

Fig. 2. The circuit model of the experimental apparatus.

A. The Resonance Method

Getsinger's effective relative permittivity measurement method [1] is based upon the resonance of a microstrip line which is short-circuited at both ends by conductive planes (shorting plates). Fig. 2 shows the experimental circuit model, consisting of a line length l, two short-circuit terminations, and two (lightly coupled) probes. In this experiment, the probe terminations Z_1 and Z_2 were chosen to be reactive. The first probe functioned as the coupler between the source of electromagnetic energy and the test microstrip, and the second probe served as a detection coupler. By using an HP 8510 automatic network analyzer and appropriate light coupling to the test microstrip line, $|S_{11}|$ near unity and very sharp but small transmission peaks ($|S_{21}|$) corresponding to system resonances could be observed. The system resonances were shown to be dominated by the true microstrip line resonances by verifying the frequency insensitivity of the transmission spikes to variations in the line couplings. Beyond the respective cutoff frequencies, higher order (nonfundamental) modes could propagate along the microstrip, complicating the ϵ_{eff} measurements slightly. Coupling to the fundamental mode was maximized while coupling to the higher order microstrip modes was suppressed. This and the application of several processing features of the HP 8510 helped separate the fundamental mode resonance peaks from the higher order mode resonance peaks.

The effective relative permittivity, which is the relative permittivity of a single-dielectric TEM transmission line whose phase velocity equals that of the microstrip line, may be easily related to the resonance measurements of the test structure. At any fundamental mode resonance, the length of the test microstrip is an integral number of half wavelengths, or

$$l = n\lambda/2 \tag{1}$$

where n is the resonance number, λ is the wavelength, and l is the microstrip length. Using the definition of ϵ_{eff} and knowing n, l, and the resonant frequency f, one may algebraically manipulate (1) into

$$\epsilon_{eff} = [nc/(2fl)]^2 \tag{2}$$

where c is the speed of light in free space. Equation (2) was used for all resonance analyses in this work.

B. The Construction Techniques

The use of large-scale circuitry and the lack of commercial circuit processing systems for these sizes necessitated the use of custom circuit constructions, which are described below [10]. Two different plating processes were used in the circuit constructions. Two microstrip substrates, one 0.245 in high $\times$ 4.719 in wide $\times$ 2.438 in long and the other 0.229 in high $\times$ 5.20 in wide $\times$ 3.02 in

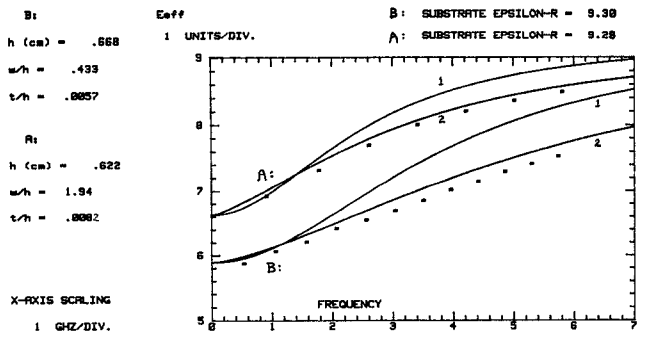

Fig. 3. Experimental results and microstrip model predictions of the effective relative permittivity ϵ_{eff} versus frequency. (1) Hammerstad and Jensen's model. (2) Kirschning and Jansen's model. At 6 GHz, $fh_A = 3.73$ GHz-cm and $fh_B = 4.0$ GHz-cm.

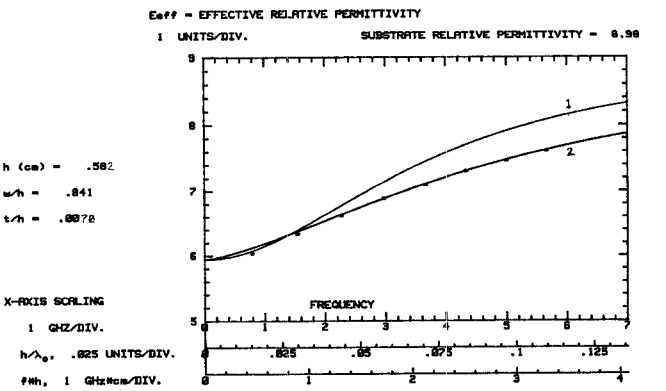

Fig. 4. Experimental results and microstrip model predictions of the effective relative permittivity ϵ_{eff} versus frequency. (1) Hammerstad and Jensen's model. (2) Kirschning and Jansen's model.

long, were completely covered by 1 μm of vapor-deposited copper followed by copper electroplating until an overall conductor thickness of 1–2 mils was reached. A three-step circuit-patterning technique was then used to form the final strip conductor geometry upon the plated substrate. This involved masking the copper surfaces to be removed, plating the exposed copper regions with tin, and exposing the surfaces to a copper etchant which did not attack the tin. Well-defined microstrip lines were produced in this manner. In contrast to the first two circuits, a third microstrip circuit was patterned directly during the plating process. On this third substrate (which measured 0.263 in high $\times$ 12.0 in wide $\times$ 4.489 in long), a removable tape masked the regions which were to remain bare. The entire structure was then plated by using an electroless copper plating procedure, producing a thin base layer over the bare substrate and the mask. A layer of electroplated copper was immediately deposited over the copper base, strengthening the entire conductive layer. After the second layer deposition, the masks (tapes) were removed, leaving the strip conductor line, the ground plane, and the plated edges in intimate contact with the substrate. Further electroplating allowed an overall (average) metallization thickness of approximately 1.6 mils to be reached. However, undesirable rough "lips" (which were estimated to be from 1–3 mils high) formed on the strip conductor as a result of the higher electric fields found near the edges of the unmasked strip during the second electroplating process. Analyses of the strip conductor thicknesses using [7] and [8] indicate that the strip lips might have shifted the ϵ_{eff} measurements obtained on this third microstrip circuit by -0.03 to -0.07, a relatively small amount. To complete the constructions of all three microstrip circuits, shorting planes 3 in high and covering the width of the substrate were formed by the soldering of copper foil to the substrate edge metallizations, leaving the circuits unshielded. Although the three substrates were cut from the same dielectric sheet, they were exposed to differing environments throughout the experiments. This allowed the nonequal absorption of chemicals (including water vapor) among those substrates, altering slightly the dielectric electromagnetic properties. Therefore, the ϵ_r of each substrate was measured using a waveguide cavity resonator technique after the substrate plating processes were completed. The measurements yielded $\epsilon_r \doteq 9$ in all cases (exact values are given on Figs. 3 and 4.).

III. Measurement Results and Error Analyses

The experimental results have been plotted in Figs. 3 and 4. The predictions of Kirschning and Jansen [7] and Hammerstad and Jensen [8] for the same microstrip parameters have been plotted for each comparison. Referring to Figs. 3 and 4, differences less than 1.8 percent, 3 percent, and 0.8 percent exist between the data and the predictions of Kirschning and Jansen, respectively. (The greater deviation of curve B, Fig. 3 from Kirschning and Jansen's model might be attributed to the model B relative dimensions. Model B featured a strip of narrow width which was constructed using the direct-pattern electroless plating technique. An analysis of [7] and [8] shows that small w/h lines display greater sensitivity to parameter fluctuations than do large w/h lines. The undesired rough lips and the resulting microstrip width and thickness variations found on model B certainly shifted the ϵ_{eff} measurements somewhat.) These dispersion measurements extend up to $fh = 4$ GHz-cm. (Kirschning and Jansen claim validity for their model to approximately $fh = 3.9$ GHz-cm.) This is well beyond the 1.6 GHz-cm frequency limits of previously published experimental data [5], [6], [9]. Clearly, the experimental measurements of ϵ_{eff} support the closed-form design equations of Kirschning and Jansen over a very large frequency span, extending from dc up to a normalized frequency of 4 GHz-cm, the highest frequency investigated. One might expect Kirschning and Jansen's design equations to predict microstrip dispersion more accurately across wide bandwidths than Hammerstad and Jensen's equations because Kirschning and Jansen employed rigorous spectral-domain dispersion solutions as a basis for their work whereas Hammerstad and Jensen used quasi-static techniques in their development. Comprehensive error analyses [10], [11] indicate that the relative uncertainties in the measurements of ϵ_{eff} are less than 3 percent at the lower frequencies ($fh < 0.5$ GHz-cm) and are between 1.4 percent and 1.7 percent at the higher frequencies ($fh = 3$ GHz-cm). Thus, the error analyses allow confidence to be placed in the experimental results.

The problems of the excitation and the propagation of undesired higher order microstrip modes must be addressed. Throughout experimentation, it was observed that the higher order modes were largely evanescent below 2 GHz-cm, while at 3 to 3 1/2 GHz-cm they could easily be excited. Thus, at frequencies above 2 GHz-cm, more attention must be paid to the geometries of the microstrip layout to avoid the undesired higher order mode excitations. At frequencies approaching and surpassing 3 GHz-cm, special care is needed to prevent these excitations. In addition, general microstrip design at normalized frequencies above 4 GHz-cm would not be recommended.

IV. Research Implications for CAD

Kirschning and Jansen's closed-form model was produced via a multidimensional curve-fitting technique with Jansen's large computer-generated data base. The good agreement of the experi-

mental data with the model [7] implies the validity of the numerical data base. Jansen's spectral-domain approach to microstrip effective relative permittivity characterization has thus been verified to be sound. This allows one to place confidence in the dispersion calculations within CAD packages employing this approach to generate a numerical data base, such as the recently introduced LINMIC [12].

V. Summary

This paper has presented high-frequency effective relative permittivity measurements of three microstrip circuits, reaching a normalized frequency of 4 GHz-cm (which is higher than previously reported bandwidths in [5], [6], and [9]). These data have been compared to two recent closed-form microstrip models [7], [8] and show good agreement with the model proposed by Kirschning and Jansen [7] across the entire bandwidth.

Acknowledgment

The authors would like to thank Dr. E. G. Cristal and Dr. P. Szente of the Hewlett-Packard Company, Stanford Park Division.

References

[1] W. J Getsinger, "Measurement and modeling of the apparent characteristic impedance of microstrip," *IEEE Trans Microwave Theory Tech*, vol. MTT-31, pp. 624–632, Aug. 1983.

[2] M. Hashimoto, "A rigorous solution for dispersive microstrip," *IEEE Trans Microwave Theory Tech.*, vol. MTT-33, pp. 1131–1137, Nov. 1985

[3] P Pramanick and P. Bhartia, "An accurate description of dispersion in microstrip," *Microwave J.*, pp. 89–92, Dec 1983.

[4] T. Itoh and R. Mittra, "Spectral-domain approach for calculating the dispersion characteristics of microstrip lines," *IEEE Trans Microwave Theory Tech.*, vol. MTT-21, pp 496–499, July 1973.

[5] W. J. Getsinger, "Microstrip dispersion model," *IEEE Trans Microwave Theory Tech.*, vol. MTT-21, pp. 34–39, Jan. 1973.

[6] E. J. Denlinger, "A frequency dependent solution for microstrip transmission lines," *IEEE Trans. Microwave Theory Tech.*, vol. MTT-19, pp. 30–39, Jan. 1971.

[7] M. Kirschning and R. H Jansen, "Accurate model for effective dielectric constant of microstrip with validity up to millimetre-wave frequencies," *Electron. Lett.*, vol. 18, no. 6, pp. 272–273, Mar 18, 1982.

[8] E. Hammerstad and O. Jensen, "Accurate models for microstrip computer-aided design," in *1980 IEEE MTT-S Dig.*, pp. 407–409.

[9] C. P. Hartwig, D. Massé, and R. A. Pucel, "Frequency dependent behavior of microstrip," in *1968 G-MTT Int. Microwave Symp. Dig.*, pp. 110–119.

[10] S. Deibele, "Microstrip: The effective relative permittivity and the impedance," Dept of Electrical and Computer Engineering, University of Wisconsin-Madison, Rep. No ECE-86-14, July 1986

[11] S. Deibele, "Measurement of the effective relative permittivity and the apparent impedance of microstrip," presented to the Hewlett-Packard Co., Stanford Park Division, Aug. 17, 1984.

[12] R. H Jansen, "LINMIC: A CAD package for the layout-oriented design of single- and multi-layer MICs/MMICs up to mm-wave frequencies," *Microwave J.*, pp 151–161, Feb. 1986.